An introduction to OFDM – modeling and implementation

$f_k = f_0 + kf_\Delta, \quad k = 0,1,\ldots,K-1$

$f_k = f_{rc} + g_k f_\Delta, \quad k = 0,1,\ldots,K-1$

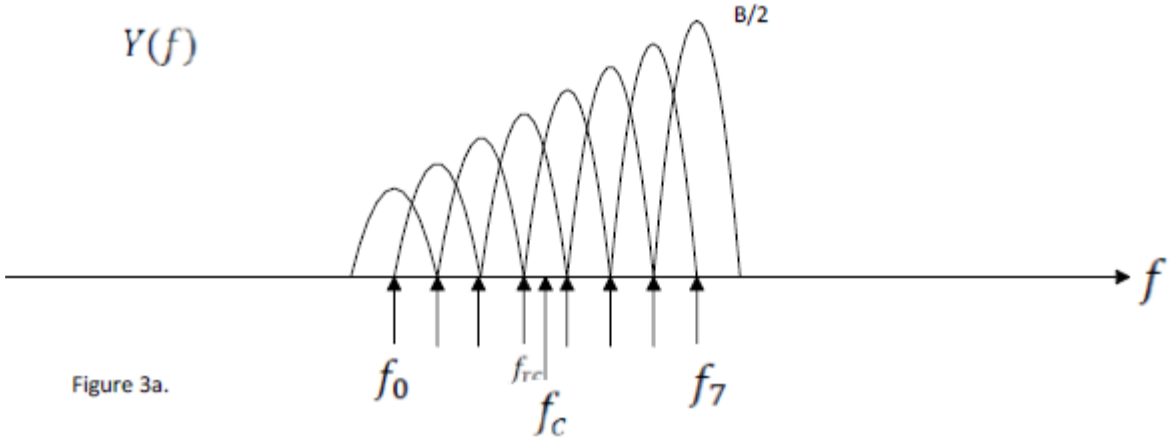

Figure 3a.

$g_0 f_\Delta, \ldots, -f_\Delta, 0, f_\Delta, \ldots\ldots, g_{K-1} f_\Delta$

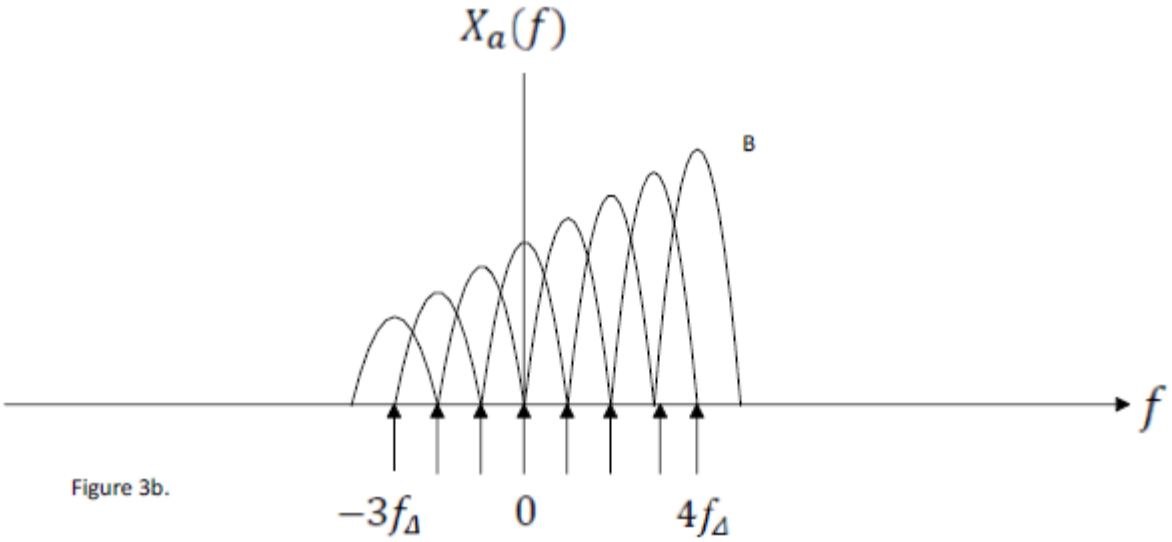

Figure 3b.

$$\text{OFDM signal(t)} = g_{rec}(t)\sum_{k=0}^{K-1} Re\{a_k e^{j2\pi f_k t}\} = g_{rec}(t)Re\{\sum_{k=0}^{K-1} a_k e^{j2\pi f_k t}\} =$$

$$= g_{rec}(t)Re\{\sum_{k=0}^{K-1} a_k e^{j2\pi(f_0+kf_\Delta)t}\} = g_{rec}(t)Re\{(\sum_{k=0}^{K-1} a_k e^{j2\pi(g_0+k)f_\Delta t})e^{j2\pi f_{rc}t}\} =$$

$$= g_{rec}(t)Re\{(\sum_{k=0}^{K-1} a_k e^{j2\pi g_k f_\Delta t})e^{j2\pi f_{rc}t}\} \qquad (1.13)$$

$$\text{OFDM signal(t)} = = g_{rec}(t)Re\{(\sum_{k=0}^{K-1} a_k e^{j2\pi(-(K-1)/2+k)f_\Delta t})e^{j2\pi f_c t}\} =$$

$$= g_{rec}(t)Re\left\{(\sum_{l=-(K-1)/2}^{(K-1)/2} a_{l+(K-1)/2} e^{j2\pi l f_\Delta t})e^{j2\pi f_c t}\right\} \quad ,K \text{ is odd} \qquad (1.14)$$

$$\text{OFDM signal(t)} = = g_{rec}(t)Re\{(\sum_{k=0}^{K-1} a_k e^{j2\pi(-(K-2)/2+k)f_\Delta t})e^{j2\pi f_{rc}t}\} =$$

$$= g_{rec}(t)Re\left\{(\sum_{l=-(K-2)/2}^{K/2} a_{l+(K-2)/2} e^{j2\pi l f_\Delta t})e^{j2\pi f_{rc}t}\right\} \quad ,K \text{ is even} \qquad (1.15)$$

$$y(t) = Re\{(\sum_{k=0}^{K-1} a_k e^{j2\pi g_k f_\Delta t}) e^{j2\pi f_{rc} t}\} = Re\{x(t) e^{j2\pi f_{rc} t}\} \qquad (2.2)$$

$$x(t) = x_{Re}(t) + j x_{Im}(t) = \sum_{k=0}^{K-1} a_k e^{j2\pi g_k f_\Delta t}, \qquad 0 \le t \le T_{obs} \qquad (2.3)$$

$$y(t) = Re\{x(t) e^{j2\pi f_{rc} t}\} = x_{Re}(t) \cos(2\pi f_{rc} t) - x_{Im}(t) \sin(2\pi f_{rc} t) \qquad (2.5)$$

$$f_{samp} = N/T_{obs} = N f_\Delta > K f_\Delta \qquad (2.12)$$

$$x_n = x(nT_{obs}/N) = \sum_{k=0}^{K-1} a_k e^{j2\pi g_k n/N} \qquad n = 0,1 \ldots, (N-1) \qquad (2.13)$$

Observe that the right hand side of Equation (2.13) actually gives us a way to create the desired samples $x_0, x_1, \ldots, x_{N-1}$ **of the complex baseband OFDM signal** $\boldsymbol{x(t)}$**!**

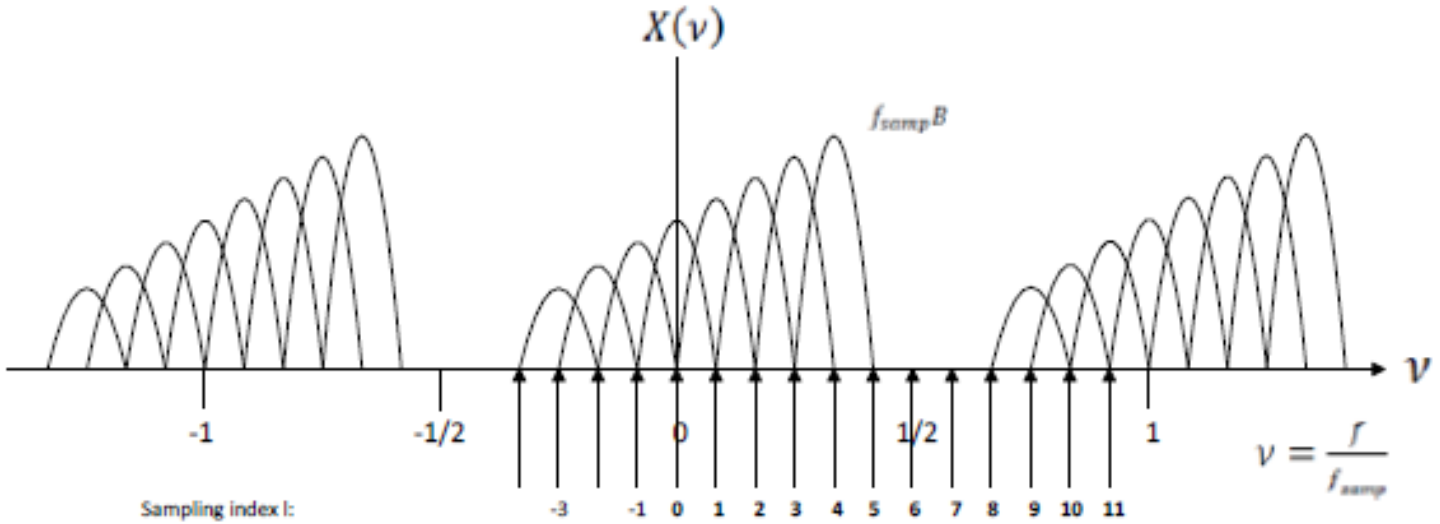

$$X(\nu) = \sum_{n=0}^{N-1} x_n e^{-j2\pi\nu n} \qquad (2.14)$$

$$X_m = X(\nu = m/N) = \sum_{n=0}^{N-1} x_n e^{-j2\pi mn/N}, \quad m = 0,1,\dots,N-1 \quad \textbf{(DFT)} \qquad (2.15)$$

$$x_n = \frac{1}{N}\sum_{m=0}^{N-1} X_m e^{j2\pi mn/N}, \quad n = 0,1,\dots,N-1 \quad \textbf{(IDFT)} \qquad (2.16)$$

Consider as an **example** the case K=8 and N=12. In this case $k_{rc} = 3$ and $g_{K-1} = 4$, and the desired sequence $X_0, X_1, \dots, X_{11}$ then equals: $Na_3, Na_4, Na_5, Na_6, Na_7, 0,0,0,0, Na_0, Na_1, Na_2$. See also Figure 6.

$$x_n = \frac{1}{N}\sum_{m=0}^{N-1} X_m e^{j2\pi mn/N}, \qquad n = 0,1,\dots,N-1 \qquad \textbf{(IDFT)} \qquad (2.16)$$

Hence, as soon as we have determined the samples in the frequency domain $X_0, X_1, \dots, X_{N-1}$ we should use them in the size-N IDFT in Equation (2.16) to create the desired sequence of time-domain samples x! *The values X_m will be determined in step 3.*

In practice, **N is chosen to be a power of 2** since fast Fourier transform (FFT) algorithms then can be used to significantly speed up the calculations in Equations (2.15) - (2.16).

Let us use Equation (2.13) to establish the connection between the sequences $a_0, a_1, \dots, a_{K-1}$ and $X_0, X_1, \dots, X_{N-1}$. We rewrite Equation (2.13) in the following way,

$$x_n = x\left(\frac{nT_{obs}}{N}\right) = \sum_{k=0}^{K-1} a_k e^{\frac{j2\pi g_k n}{N}} = \sum_{k=0}^{K-1} a_k e^{j2\pi(g_0+k)n/N} =$$

$$= \sum_{k=0}^{-g_0-1} a_k e^{j2\pi(g_0+k+N)n/N} + \sum_{k=-g_0}^{K-1} a_k e^{j2\pi(g_0+k)n/N} =$$

$$= \sum_{m=g_0+N}^{N-1} a_{m-(g_0+N)} e^{j2\pi mn/N} + \sum_{m=0}^{g_{K-1}} a_{m-g_0} e^{j2\pi mn/N} =$$

$$= \frac{1}{N}\sum_{m=0}^{N-1} X_m e^{j2\pi mn/N} \qquad (2.18)$$

Inspection of Equation (2.18) yields the relationships below:

$$X_m = N a_{m-g_0}, \quad \text{if} \quad 0 \le m \le g_{K-1} \qquad (2.19)$$

$$X_m = 0, \quad \text{if} \quad g_{K-1} + 1 \le m \le g_0 + N - 1 \qquad (2.20)$$

$$X_m = N a_{m-(g_0+N)}, \text{ if} \quad g_0 + N \le m \le N - 1 \qquad (2.21)$$

As an **example:** Consider the WLAN standard IEEE 802.11n, see the example on page 7. Since K=117 then $k_{rc} = -g_0 = \frac{K-1}{2} = 58$ and $g_{K-1} = \frac{K-1}{2} = 58$. Furthermore, assume that N=128. From Equations (2.19) – (2.21) it is then concluded that the sub-sequence $X_0, X_1, \ldots, X_{58}$ contains the QAM signal points $a_{58}, a_{59}, \ldots, a_{116}$, the sub-sequence $X_{59}, X_{60}, \ldots, X_{69}$ contains only zero values, and the sub-sequence $X_{70}, X_{71}, \ldots, X_{127}$ contains the QAM signal points $a_0, a_1, \ldots, a_{57}$.

$$X_l = Na_{k_{rc}+l} \qquad l = 0,1 \ldots, g_{K-1} \tag{2.27}$$

$$X_{-k_{rc}+N+k} = Na_k \qquad k = 0,1, \ldots (k_{rc} - 1) \tag{2.29}$$

If we first construct the size-N sequence $Na_0, Na_1, \ldots, Na_{K-1}, 0,0, \ldots,0$, and then "left-rotate" this sequence n_{rc} positions (or "right-rotate" this sequence $(g_0 + N)$ positions), then the desired sequence $X_0, X_1, \ldots, X_{N-1}$ in equations (2.20)-(2.25) is obtained!

Consider as an **example** the case K=8 and N=12. In this case $k_{rc} = 3$ and $g_{K-1} = 4$, and the desired sequence $X_0, X_1, \ldots, X_{11}$ then equals: $Na_3, Na_4, Na_5, Na_6, Na_7, 0,0,0,0, Na_0, Na_1, Na_2$. See also Figure 6.

The final step is to calculate the size-N **IDFT**,

$$x_n = \frac{1}{N}\sum_{m=0}^{N-1} X_m e^{j2\pi mn/N}, \qquad n = 0,1,\dots,N-1 \qquad (2.30)$$

In practice, **N is chosen to be a power of 2** since fast Fourier transform (FFT) algorithms can then be used to significantly speed up the calculations in equation (2.30).

Equation (2.30) is the desired final expression to compute the discrete-time signal x, i.e. the N time-domain samples of the complex baseband OFDM signal $\boldsymbol{x(t)}$. Equation (2.30), i.e. the size-N IDFT, is computationally very efficient when implemented using FFT algorithms (if N is chosen to be a power of 2). The sequence $\boldsymbol{X_0, X_1, \dots, X_{N-1}}$ is given by Equations (2.27) and (2.29) or alternatively by Equations (2.19)-(2.21). See also the construction ("rotation") given above. See also Figure 7 on page 27.

The $(N-K)$ zeroes in the sequence $X_0, X_1, \dots, X_{N-1}$ may be interpreted as using zero-valued signal-points at baseband sub-carrier frequencies located at the edges but outside of the OFDM frequency band.

3. The Cyclic Prefix (CP) and Digital-to-Analog (D/A) conversion

Based on the discussion about periodicity above let us therefore construct a new size-(L+N) vector $\boldsymbol{u}$ as a so-called *periodic extension* of the size-N vector **x**. This means that *the L last samples in* $\boldsymbol{x}$ *are copied and placed as the first L samples in* $\boldsymbol{u}$. The remaining N samples in $\boldsymbol{u}$ are identical to $\boldsymbol{x}$. This means that,

$$u_0 = x_{N-L}, \ldots, u_{L-1} = x_{N-1}, u_L = x_0, \ldots, u_{L+N-1} = x_{N-1}. \quad (3.1)$$

The construction of the vector $\boldsymbol{u}$ above implies that the first L samples in $\boldsymbol{u}$ are identical with the last L samples in $\boldsymbol{u}$, and this reflects the periodicity discussed above.

The duration of the OFDM signal interval is T_s, and it can be expressed as,

$$T_s = \frac{(L+N)T_{obs}}{N} = T_{CP} + T_{obs} \quad (3.2)$$

The vector $\mathbf{u}$ in equation (3.1) contains (L+N) time-domain complex samples of a complex baseband OFDM signal defined over the entire OFDM signal interval $0 \leq t \leq T_s$. This complex baseband OFDM signal is here denoted $\mathbf{u}(t)$, and based on the previous discussion in this section, the OFDM signal $\mathbf{u}(t)$ is,

$$u(t) = u_{Re}(t) + ju_{Im}(t) = \sum_{k=0}^{K-1} a_k e^{j2\pi g_k f_\Delta (t - T_{CP})}, \quad 0 \leq t \leq T_s \tag{3.3}$$

$$s(t) = Re\{u(t)e^{j2\pi f_{rc} t}\} = u_{Re}(t)\cos(2\pi f_{rc} t) - u_{Im}(t)\sin(2\pi f_{rc} t) \tag{3.5}$$

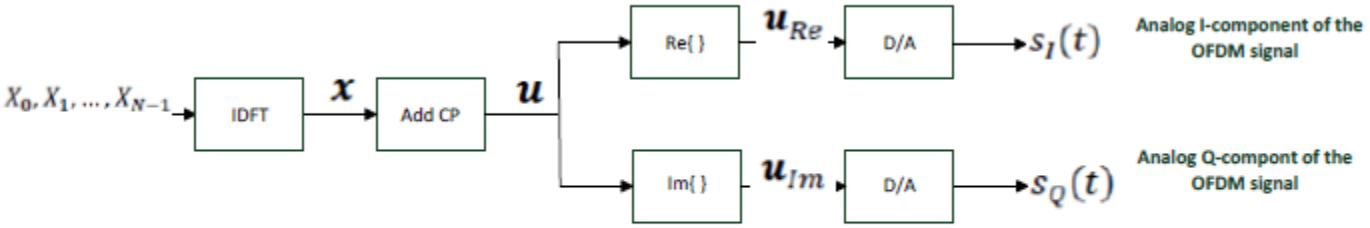

Figure 7. Block diagram illustrating the operations in the digital domain, and the transition to the analog domain. The IDFT is given in Equation (2.30) (and in Equation (2.18)).

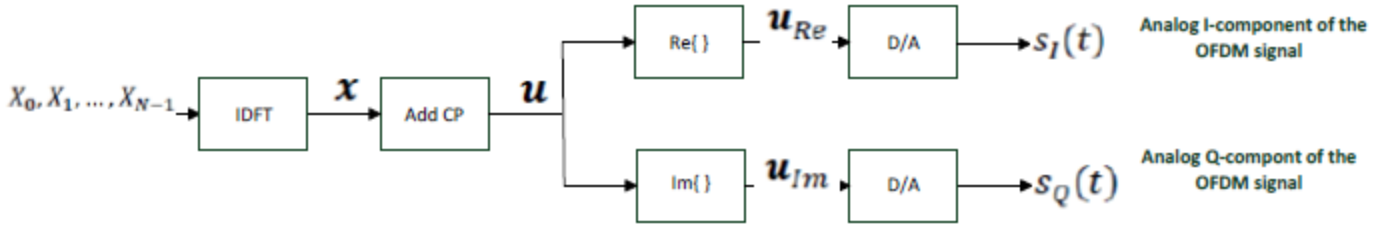

Figure 7. Block diagram illustrating the operations in the digital domain, and the transition to the analog domain. The IDFT is given in Equation (2.30) (and in Equation (2.18)).

$$s(t) = s_I(t)\cos(2\pi f_{rc}t + \phi) - s_Q(t)\sin(2\pi f_{rc}t + \phi) \qquad (4.1)$$

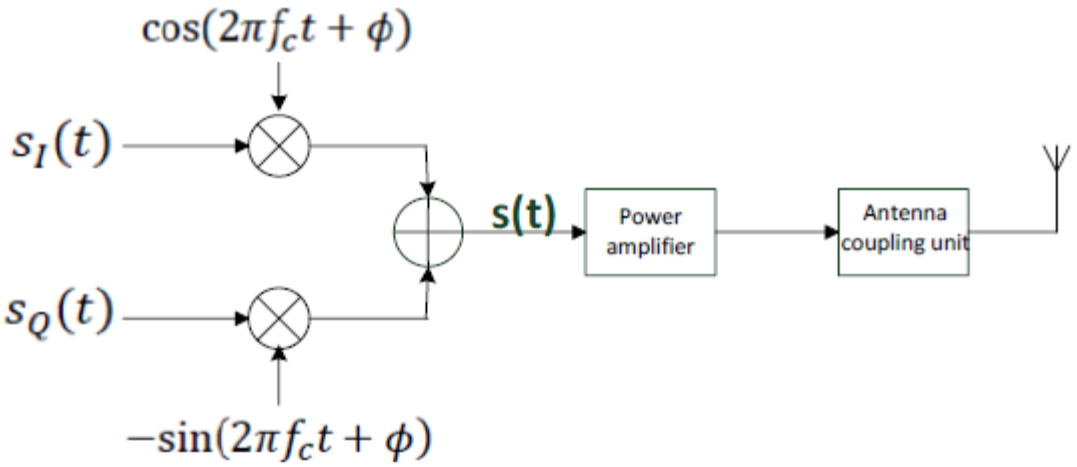

Figure 8. Block diagram illustrating frequency up-conversion (mixer stage) to the carrier frequency (K is odd), the power amplifier, and the antenna coupling unit. The OFDM signal $s(t)$ is given in Equation (4.1).

Section 5: The multi-path (linear filter) channel, and the additive white Gaussian noise (AWGN)

INPUT OFDM: $As(t) = ARe\left\{\left(\sum_{k=0}^{K-1} a_k e^{j2\pi g_k f_\Delta (t-T_{CP})}\right) e^{j(2\pi f_{rc} t+\phi)}\right\}, \quad 0 \le t \le T_s$ (5.10)

or alternatively as,

INPUT OFDM: $As(t) = ARe\left\{\sum_{k=0}^{K-1} a_k\, e^{j(2\pi f_k t+\theta_k)}\right\}, \qquad 0 \le t \le T_s$ (5.11)

OUTPUT OFDM: $z(t) = ARe\left\{\left(\sum_{k=0}^{K-1} a_k H(f_k) e^{j2\pi g_k f_\Delta (t-T_{CP})}\right) e^{j(2\pi f_{rc} t+\phi)}\right\}, \quad T_{CP} \le t \le T_s$ (5.12)

or alternatively as,

OUTPUT OFDM: $z(t) = ARe\left\{\sum_{k=0}^{K-1} a_k H(f_k)\, e^{j(2\pi f_k t+\theta_k)}\right\}, \qquad T_{CP} \le t \le T_s$ (5.13)

6. The Receiver: Frequency down-converting, sampling (A/D) and the DFT

$$r(t) = b_I \cos(2\pi f_B t) - b_Q \sin(2\pi f_B t) + n(t)\,,\ 0 \le t \le T$$

$$\psi_1(t) = \cos(2\pi f_B t)/C\,, \qquad 0 \le t \le T$$

$$\psi_2(t) = -\sin(2\pi f_B t)/C\,, \qquad 0 \le t \le T$$

$$r_1 = \int_0^T r(t)\psi_1(t)\,dt = Cb_I + n_1 \qquad r_2 = \int_0^T r(t)\psi_2(t)\,dt = Cb_Q + n_2$$

$$r = r_1 + jr_2 = \int_0^T r(t)e^{-j2\pi f_B t}\,dt/C = R(f_B)/C = Cb + n \qquad (6.8)$$

It is now very important to observe in equation (6.8) that **the received noisy signal point r can be found by calculating the Fourier transform $R(f)$ of the received signal $r(t)$ over the time interval $0 \le t \le T$, and then sample $R(f)$ at $f = f_B$ to obtain $R(f_B)$.** As will be seen later on, *using the DFT in an OFDM receiver can be viewed as a natural extension of this result.* This concludes the example, and it is time to focus on frequency down-converting to baseband.

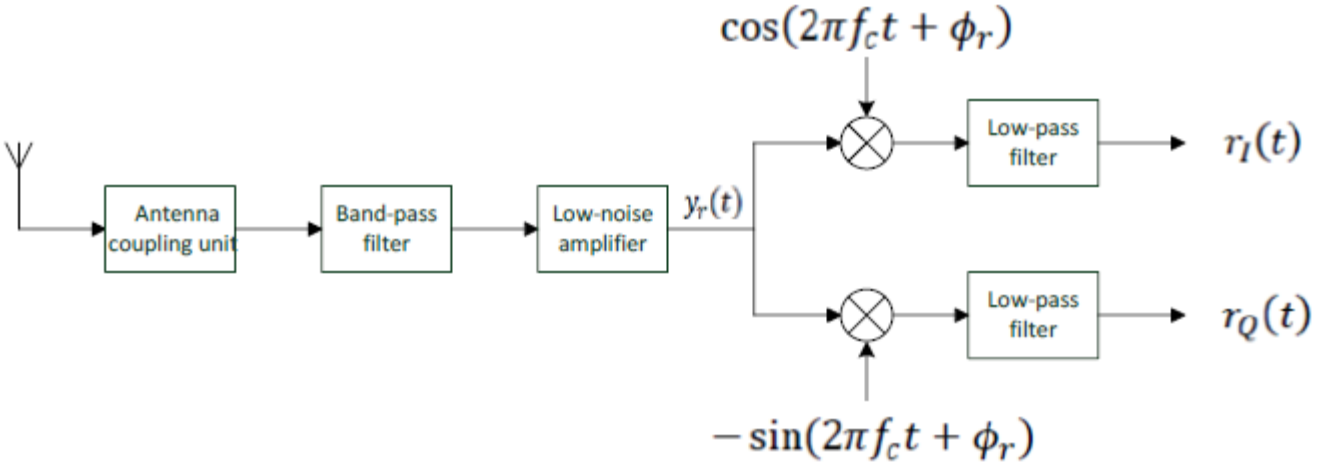

Figure 10. Illustrating the first part of the receiver: the antenna coupling unit, band-pass filter, low-noise amplifier (LNA) and a homodyne unit for frequency down-conversion and extracting the baseband signals $r_I(t)$ and $r_Q(t)$. It is here assumed that K is odd for which $f_{rc} = f_c$.

$$r_I(t) + jr_Q(t) = \sum_{k=0}^{K-1} a_k H_{eq}(f_k) e^{j2\pi g_k f_\Delta (t - T_{CP})} + w(t), \quad T_{CP} \le t \le T_s \tag{6.15}$$

$$H_{eq}(f_k) = H_{eq,k} = AH(f_k) e^{j\phi} G_1(f_k) e^{-j\phi_r} G_{lp}(f_k - f_{rc} = g_k f_\Delta)/2 \tag{6.16}$$

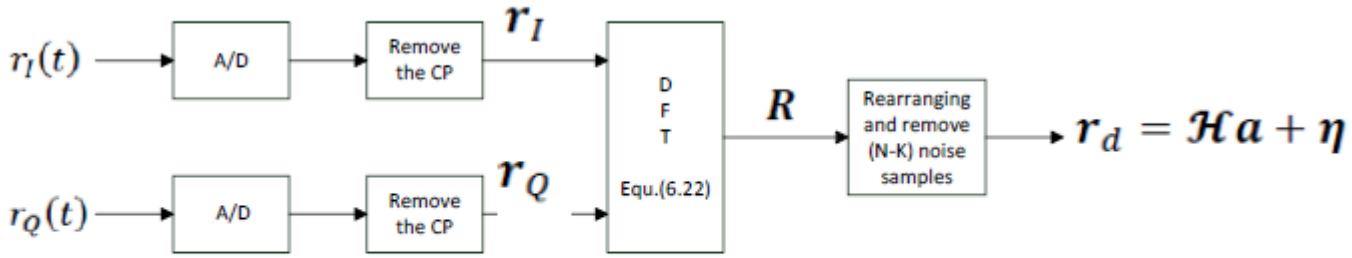

Figure 11. Illustrating sampling, removal of the CP, and the size-N DFT in the receiver to extract the K received distorted and noisy signal points collected in the size-K vector $\boldsymbol{r}_d$.

$$r_{I,n} = r_I((L+n)T_{obs}/N), \quad n = 0,1,\dots,N-1 \tag{6.17}$$

$$r_{Q,n} = r_Q((L+n)T_{obs}/N), \quad n = 0,1,\dots,N-1 \tag{6.18}$$

$$\boldsymbol{r} = \boldsymbol{r}_I + j\boldsymbol{r}_Q \tag{6.19}$$

$$R(\nu) = \sum_{n=0}^{N-1} r_n e^{-j2\pi\nu n} \tag{6.21}$$

$$R_m = R(\nu = m/N) = \sum_{n=0}^{N-1} r_n e^{-j2\pi mn/N}, \quad m = 0,1,\dots,N-1 \tag{6.22}$$

$$\boldsymbol{R} = \boldsymbol{X}_r + \boldsymbol{w}_r \qquad (6.24)$$

$$(\mathcal{H}\boldsymbol{a})^{tr} = (a_0 H_{eq,0} \;\; a_1 H_{eq,1} \ldots . a_{K-1} H_{eq,K-1}) \qquad (6.25)$$

$$\boldsymbol{X}_r = N\boldsymbol{Q}_t \mathcal{H}\boldsymbol{a} \qquad (6.26)$$

$$\boldsymbol{r}_d = \frac{1}{N}\boldsymbol{Q}_r \boldsymbol{R} = \boldsymbol{Q}_r \boldsymbol{Q}_t \mathcal{H}\boldsymbol{a} + \frac{1}{N}\boldsymbol{Q}_r \boldsymbol{w}_r = \mathcal{H}\boldsymbol{a} + \boldsymbol{\eta} \qquad (6.28)$$

Observe that the elements in the size-K column vector $\boldsymbol{r}_d$ in Equation (6.28) are the desired received distorted and noisy signal points,

$$r_{d,k} = a_k H_{eq,k} + \eta_k, \qquad k = 0,1, \ldots, (K-1) \qquad (6.29)$$

The results in Equations (6.28)-(6.29) are extremely important!

For the special case of *uncoded* OFDM (though rarely used in practice)

$$P_{s,k} = 4\left(1 - \frac{1}{\sqrt{M_k}}\right) Q\left(\sqrt{\frac{d_{min,k}^2 \mathcal{E}_{b,k}}{N_0}}\right) - 4\left(1 - \frac{1}{\sqrt{M_k}}\right)^2 Q^2\left(\sqrt{\frac{d_{min,k}^2 \mathcal{E}_{b,k}}{N_0}}\right), \quad k = 0,1 \ldots, K-1 \quad (6.30)$$

where $d_{min,k}^2$ is the normalized squared minimum Euclidean distance in the received QAM signal constellation with index k and,

$$d_{min,k}^2 = \frac{3log_2(M_k)}{M_k - 1} \quad (6.31)$$

Furthermore, $\mathcal{E}_{b,k}$ denotes the average received signal energy per information bit in the received QAM signal space with index k, and $\mathcal{E}_{b,k}$ is proportional to $|H_{eq,k}|^2$.

Chapter 9

An Introduction to Time-varying Multipath Channels

$$\boxed{z(t) = \sum_n \alpha_n(t) s(t - \tau_n(t))} \qquad (9.1)$$

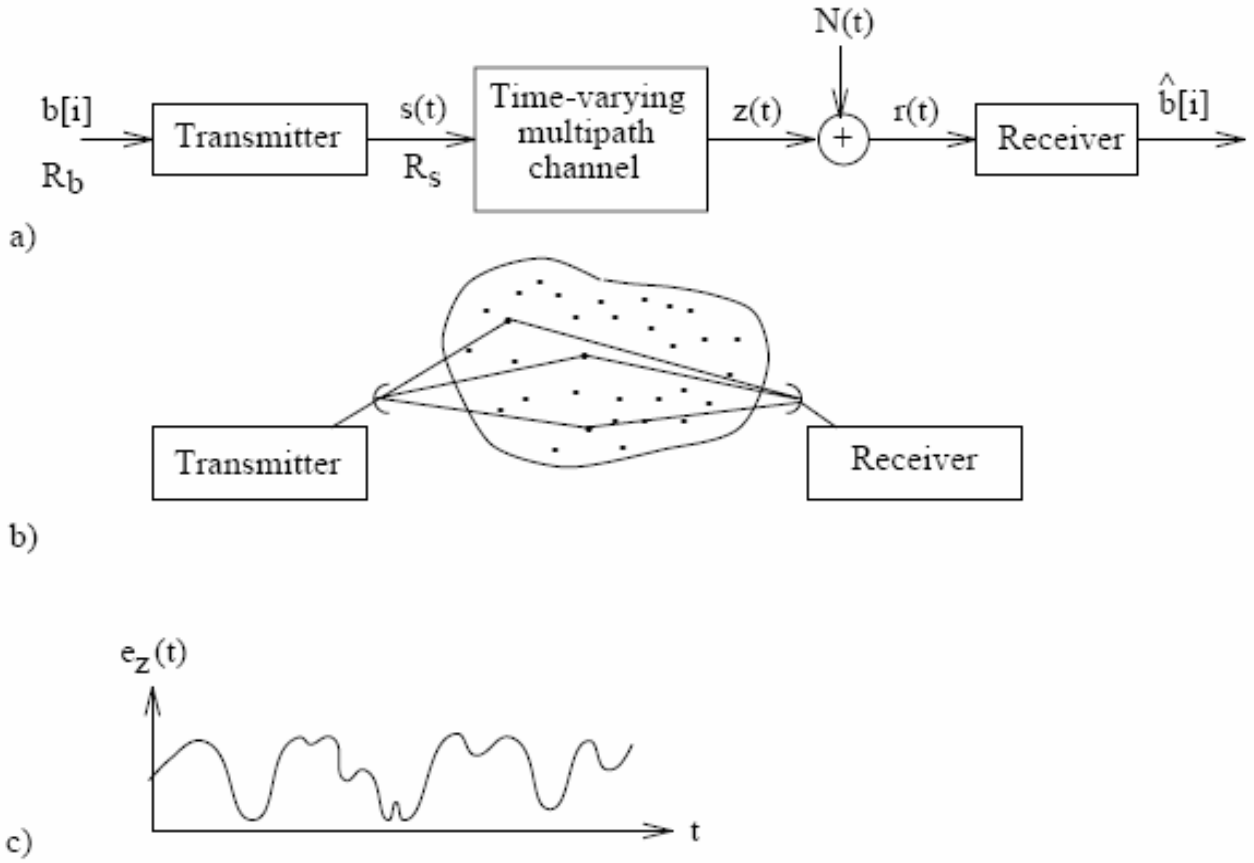

Figure 9.1: a) The digital communication system; b) A scattering medium; c) Illustrating the fading envelope $e_z(t)$.

$$s(t) = \cos((\omega_c + \omega_1)t) \ , \quad -\infty \leq t \leq \infty \tag{9.2}$$

$$\begin{aligned}
z(t) &= \sum_n \alpha_n(t) \cos((\omega_c + \omega_1)(t - \tau_n(t))) = \\
&= \underbrace{\left[\sum_n \alpha_n(t) \cos((\omega_c + \omega_1)\tau_n(t))\right]}_{z_I(t) = \tilde{H}_{Re}(f_1,t)/2} \cos((\omega_c + \omega_1)t) - \\
&\quad - \underbrace{\left[\sum_n \alpha_n(t) \sin(-(\omega_c + \omega_1)\tau_n(t))\right]}_{z_Q(t) = \tilde{H}_{Im}(f_1,t)/2} \sin((\omega_c + \omega_1)t) \\
&= z_I(t) \cos((\omega_c + \omega_1)t) - z_Q(t) \sin((\omega_c + \omega_1)t) \\
&= e_z(t) \cos((\omega_c + \omega_1)t + \theta_z(t)) \qquad (9.3)
\end{aligned}$$

Compare with the time-invariant QAM-result:

$$\begin{aligned}
A_z + jB_z &= (A + jB)H(f_c) = \sqrt{A^2 + B^2}|H(f_c)|e^{j(\nu + \phi(f_c))} = \\
&= (A + jB)(H_{Re}(f_c) + jH_{Im}(f_c)) \qquad (3.110)
\end{aligned}$$

$$s(t) = \cos((\omega_c + \omega_1)t) \ , \quad -\infty \leq t \leq \infty \tag{9.2}$$

$$\begin{aligned} z(t) &= \sum_n \alpha_n(t) \cos((\omega_c + \omega_1)(t - \tau_n(t))) = \\ &= e_z(t) \cos((\omega_c + \omega_1)t + \theta_z(t)) \end{aligned} \tag{9.3}$$

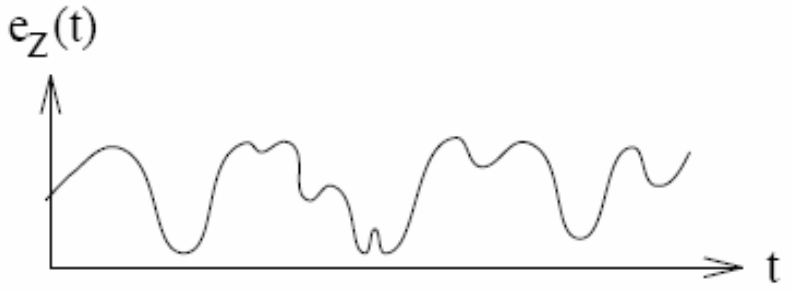

Observe that the quadrature components $z_I(t)$ and $z_Q(t)$ in (9.3) are *time-varying*. Hence, the output signal $z(t)$ is *not* a pure sine wave with frequency $f_c + f_1$. ***This is a significant difference compared with the linear time-invariant channel.*** It is seen in (9.3) that the quadrature components depend

$$z(t) = \sum_n \alpha_n(t)\cos((\omega_c+\omega_1)(t-\tau_n(t))) =$$

$$= z_I(t)\cos((\omega_c+\omega_1)t) - z_Q(t)\sin((\omega_c+\omega_1)t)$$

$$= e_z(t)\cos((\omega_c+\omega_1)t+\theta_z(t))$$

Throughout this chapter it is assumed that $z_I(t)$ and $z_Q(t)$ may be modelled as baseband zero-mean wide-sense-stationary (WSS) *Gaussian random processes* (with variances $\sigma_I^2 = \sigma_Q^2 = \sigma^2$). This is a commonly used assumption when the number of scatterers is large, implying that central limit theorem arguments can be used [43], [65], [68], [39]. For a fixed value of t, this assumption leads to a Rayleigh-distributed envelope $e_z(t)$,

$$e_z(t) = \sqrt{z_I^2(t) + z_Q^2(t)} \tag{9.4}$$

$$p_{e_z}(x) = \frac{2x}{b}\, e^{-x^2/b}, \quad x \geq 0\ , \text{ Rayleigh distr.} \tag{9.5}$$

$$b = E\{e_z^2(t)\} = 2\sigma^2 = 2P_z \tag{9.6}$$

and a uniformly distributed phase $\theta_z(t)$ (over a 2π interval). The zero-mean assumption means that there is no deterministic signal path present in $z(t)$. If a

9.1.1 Doppler Power Spectrum and Coherence Time

$$
\begin{aligned}
&R_{\mathcal{D}}(f) = \mathcal{F}(\tilde{c}_z(\tau)) \\
&\tilde{c}_z(\tau) = \frac{1}{2}\, E\{[z_I(t+\tau) + jz_Q(t+\tau)]\ [z_I(t) - jz_Q(t)]\} \\
&R_z(f) = \frac{1}{2}\, (R_{\mathcal{D}}(f + f_c + f_1) + R_{\mathcal{D}}(f - f_c - f_1))
\end{aligned}
\tag{9.7}
$$

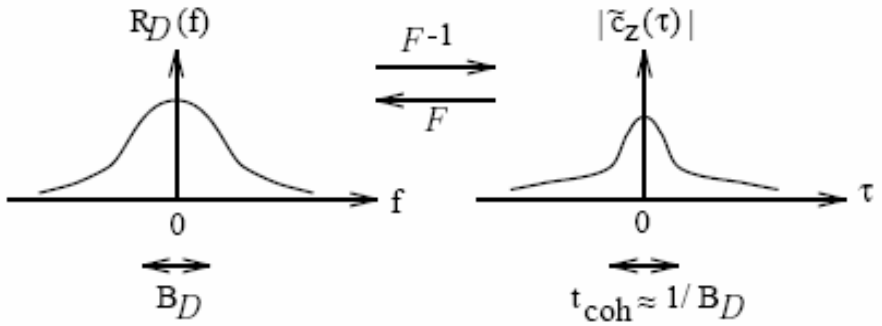

Figure 9.2: Illustrating the Fourier transform pair $\tilde{c}_z(\tau) \longleftrightarrow R_{\mathcal{D}}(f)$.

$$
t_{coh} \approx 1/B_{\mathcal{D}} \tag{9.8}
$$

If the channel is slowly changing, then the coherence time is large. Note that $z_I(t+\tau)$ and $z_I(t)$ (also $z_Q(t+\tau)$ and $z_Q(t)$) are correlated over time-intervals τ (much) smaller than the coherence time t_{coh}. Hence, input signals within such intervals are therefore affected similarly by the fading channel. On the other hand, input signals that are separated in time by (much) more than t_{coh}, are affected differently by the channel, and at the output of the channel they become essentially independent of each other. If the former case apply (time flat fading), for a given time-interval, then we say that the channel is **time-nonselective**, and if the latter case apply, then the channel is said to be **time-selective**.

9.1.2 Coherence Bandwidth and Multipath Spread

$$z(t) = z(f_1, t) = \underbrace{\frac{1}{2}\,\tilde{H}_{Re}(f_1, t)}_{z_I(t)} \cos((\omega_c + \omega_1)t) - \underbrace{\frac{1}{2}\,\tilde{H}_{Im}(f_1, t)}_{z_Q(t)} \sin((\omega_c + \omega_1)t) \tag{9.9}$$

What can be said about the output signal $z(t)$ if another frequency $f_2 = f_1 + f_\Delta$ is used, instead of f_1? Are different frequency-intervals, in the input signal spectrum, treated differently by the time-varying multipath channel? To answer these questions the correlation between $z(f_1, t)$ and $z(f_1 + f_\Delta, t)$ can be found by

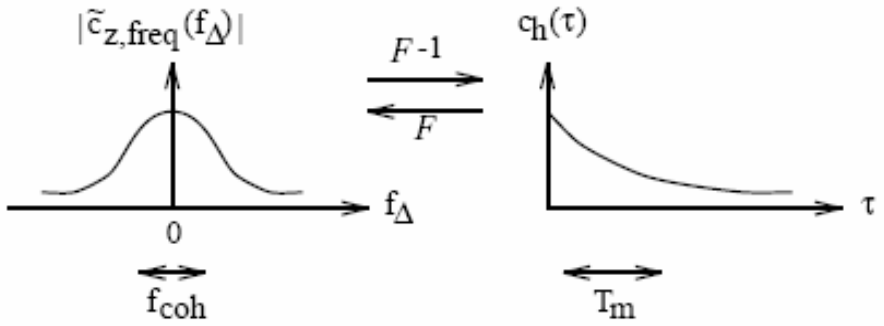

Figure 9.3: Illustrating the Fourier transform pair $c_h(\tau) \longleftrightarrow \tilde{c}_{z,freq}(f_\Delta)$.

The **coherence bandwidth** f_{coh} of the channel is defined as the width of the autocorrelation function $\tilde{c}_{z,freq}(f_\Delta)$, see Figure 9.3. Note that frequencies within a frequency-interval (much) smaller than the coherence bandwidth f_{coh} are correlated, and they are affected similarly by the fading channel. On the other hand, two frequencies that are separated by (much) more than f_{coh}, are affected differently by the channel, and they are essentially independent of each other. If the former case apply (frequency flat fading), for a given frequency-interval, then we say that the channel is **frequency-nonselective**, and if the latter case apply, then the channel is said to be **frequency-selective**.

$$z(t) = \int_{-\infty}^{\infty} h(\tau, t)s(t-\tau)d\tau \qquad (9.10)$$

delay power spectrum $c_h(\tau)$ (also multipath intensity profile) of the time-varying impulse response $h(\tau, t)$,

$$c_h(\tau) = E\left\{\frac{h^2(\tau,t)}{2}\right\} = \frac{1}{2}\,E\{h_I^2(\tau,t) + h_Q^2(\tau,t)\} = \frac{1}{2}\,E\{\tilde{h}(\tau,t)\tilde{h}^*(\tau,t)\} \quad (9.15)$$

An example of the delay power spectrum $c_h(\tau)$ is illustrated in Figure 9.3. The width of the delay power spectrum is referred to as the **multipath spread** of the channel and it is denoted by T_m. This is an important parameter since if T_m is too large, compared with e.g. the symbol time, then intersymbol interference can occur.

$$T_m \approx 1/f_{coh} \qquad (9.16)$$

9.2 Frequency-Nonselective, Slowly Fading Channel

$$T_s \ll t_{coh} \tag{9.27}$$

or equivalently,

$$B_{\mathcal{D}} \ll R_s \tag{9.28}$$

This means that the channel is **slowly fading**, which imply that it can be treated as a time-invariant channel within the coherence time.

In this subsection a frequency-nonselective channel is investigated. To obtain this situation it is required that the bandwidth of the transmitted signal, denoted W, is much smaller than the coherence bandwidth f_{coh} of the channel,

$$W \ll f_{coh} \tag{9.29}$$

or equivalently,

$$T_m \ll 1/W \tag{9.30}$$

$$\tilde{z}(t) = \frac{1}{2}\int_{-\infty}^{\infty} \tilde{S}(f)\tilde{H}(f,t)e^{j2\pi ft}df \qquad (9.26)$$

$$z_I(t) + jz_Q(t) = \frac{1}{2}\int_{-\infty}^{\infty} [S_I(f) + jS_Q(f)]\ [H_I(f,t) + jH_Q(f,t)]e^{j2\pi ft}df \qquad (9.33)$$

$$z_I(t) + jz_Q(t) = \frac{1}{2}\int_{-\infty}^{\infty} [S_I(f) + jS_Q(f)] \cdot (H_I + jH_Q)e^{j2\pi ft}df \qquad (9.36)$$

$$\begin{aligned} z_I(t) + jz_Q(t) &= \frac{1}{2}\,(s_I(t) + js_Q(t))(H_I + jH_Q) = \\ &= e_s(t)e^{j\theta_s(t)} \cdot ae^{j\phi} = e_z(t)e^{j\theta_z(t)} \end{aligned} \qquad (9.37)$$

$$
\begin{aligned}
z_I(t) + jz_Q(t) &= \frac{1}{2}\,(s_I(t) + js_Q(t))(H_I + jH_Q) = \\
&= e_s(t)e^{j\theta_s(t)} \cdot ae^{j\phi} = e_z(t)e^{j\theta_z(t)} \qquad (9.37)
\end{aligned}
$$

$$
\boxed{\boxed{z(t) = ae_s(t)\cos(\omega_c t + \theta_s(t) + \phi)}} \qquad (9.38)
$$

$$
p_a(x) = \frac{2x}{b}\, e^{-x^2/b}, \quad x \geq 0 \quad \text{(Rayleigh distribution)} \qquad (9.39)
$$

where,

$$
\begin{aligned}
E\{a\} &= \frac{1}{2}\,\sqrt{\pi b} \qquad (9.40)\\
E\{a^2\} &= b \qquad (9.41)
\end{aligned}
$$

and,

$$
p_\phi(y) = \begin{cases} 1/2\pi & , \quad -\pi \leq y \leq \pi \\ 0 & , \quad \text{otherwise} \end{cases} \qquad (9.42)
$$

If we assume uncoded equally likely binary signals over a Rayleigh fading channel ($z_1(t) = as_1(t), z_0(t) = as_0(t)$), then the bit error probability of the ideal coherent ML receiver is ($0 < d^2 = \frac{D^2_{s_1,s_0}}{2E_{b,sent}} \leq 2$)

$$\boxed{P_b = \int_0^\infty \Pr\{\text{error}|a\} p_a(x) dx = E\{\Pr\{\text{error}|a\}\}} \qquad (9.43)$$

$$\begin{aligned}
P_b &= \int_0^\infty Q(\sqrt{d^2 x^2 E_{b,sent}/N_0}) \; \frac{2x}{b} \; e^{-x^2/b} dx = \\
&= -e^{-x^2/b} \; Q(x\sqrt{d^2 E_{b,sent}/N_0})\Big]_0^\infty - \int_0^\infty (-e^{-x^2/b}) \\
&\left(\frac{-\sqrt{d^2 E_{b,sent}/N_0}}{\sqrt{2\pi}} \; e^{-\frac{x^2 d^2 E_{b,sent}/N_0}{2}} \right) dx = \\
&= \frac{1}{2} - \sqrt{d^2 E_{b,sent}/N_0} \cdot \beta \underbrace{\int_0^\infty \frac{e^{-x^2/2\beta^2}}{\beta\sqrt{2\pi}} dx}_{1/2} \qquad (9.44)
\end{aligned}$$

$$\mathcal{E}_b = E\{a^2\}E_{b,sent} = bE_{b,sent} \tag{9.45}$$

$$P_b = \frac{1}{2}\left(1 - \sqrt{\frac{d^2\mathcal{E}_b/N_0}{2 + d^2\mathcal{E}_b/N_0}}\right) = \frac{1}{2 + d^2\mathcal{E}_b/N_0 + \sqrt{2 + d^2\mathcal{E}_b/N_0}\sqrt{d^2\mathcal{E}_b/N_0}}$$

$$\begin{array}{ll} \mathcal{E}_b/N_0 \text{ “large”} & \\ \downarrow & \\ \approx & \dfrac{1}{2d^2\mathcal{E}_b/N_0} \end{array} \tag{9.46}$$

where $d^2 = 2$ for antipodal signals and $d^2 = 1$ for orthogonal signals.
Observe the dramatic increase in P_b due to the Rayleigh fading channel. P_b is no longer exponentially decaying in $\mathcal{E}_b/N_0$, it now decays essentially as $(\mathcal{E}_b/N_0)^{-1}$!

EXAMPLE 9.1

Assume that equally likely, binary orthogonal FSK signals, with equal energy, are sent from the transmitter. Hence, $s_i(t) = \sqrt{2E_{b,sent}/T_b}\cos(2\pi f_i t)$ *in* $0 \leq t \leq T_b$, $i = 0, 1$.

These signals are communicated over a Rayleigh fading channel, i.e. the received signal is (see (9.38)),

$$r(t) = a\sqrt{2E_{b,sent}/T_b}\cos(2\pi f_i t + \phi) + N(t)$$

Assume that the incoherent receiver in Figure 5.28 on page 397 is used. From (5.109) it is known that for a given value of a,

$$P_b = \frac{1}{2}\, e^{-a^2 E_{b,sent}/2N_0}$$

since $a^2 E_{b,sent}$ *then is the average received energy per bit.*

For the Rayleigh fading channel, and the same receiver, P_b *can be calculated by using (9.43),*

$$\boxed{P_b = \int_0^\infty \Pr\{error|a = x\}p_a(x) = E\{\Pr\{error|a\}\}}$$

$$E\{\Pr\{error|a\}\} = E\left\{\frac{1}{2}\ e^{-a^2 E_{b,sent}/2N_0}\right\} =$$

$$E\left\{\frac{1}{2}\ e^{-a_1^2 E_{b,sent}/2N_0}\right\} \cdot E\left\{e^{-a_2^2 E_{b,sent}/2N_0}\right\}$$

$$P_b = \frac{1/2}{1 + \frac{E_{b,sent}}{N_0} \cdot \frac{E\{a^2\}}{2}} = \frac{1}{2 + \mathcal{E}_b/N_0}$$

Observe the dramatic increase in P_b due to the Rayleigh fading channel. P_b is no longer exponentially decaying in $\mathcal{E}_b/N_0$, it now decays essentially as $(\mathcal{E}_b/N_0)^{-1}$! *As an example, assuming $\mathcal{E}_b/N_0 = 1000$ (30 dB), we obtain*

$$P_b = \begin{cases} 0.5e^{-500} \approx 3.6 \cdot 10^{-218} & , \quad AWGN \\ (1002)^{-1} \approx 10^{-3} & , \quad Rayleigh{+}AWGN \end{cases}$$

DIVERSITY IS NEEDED!